NANO EXPRESS

Synthesis and Characterization of Core-shell ZrO$_2$/PAAEM/PS Nanoparticles

J. Wang · T. J. Shi · X. C. Jiang

Abstract This work demonstrates the synthesis of core-shell ZrO$_2$/PAAEM/PS nanoparticles through a combination of sol–gel method and emulsifier-free emulsion polymerizaiton. By this method, the modified nanometer ZrO$_2$ cores were prepared by chemical modification at a molecular level of zirconium propoxide with monomer of acetoacetoxyethylmethacrylate (AAEM), and then copolymerized with vinyl monomer to form uniform-size hybrid nanoparticles with diameter of around 250 nm. The morphology, composition, and thermal stability of the core-shell particles were characterized by various techniques including transmission electron microscopy (TEM), X-ray diffractometer (XRD), Fourier transform infrared spectroscopy (FTIR), X-ray photoelectron spectroscopy (XPS), and thermal-gravimetry analyzer (TGA). The results indicate that the inorganic–organic nanocomposites exhibit good thermal stability with the maximum decomposition temperature of ∼447 °C. This approach would be useful for the synthesis of other inorganic–organic nanocomposites with desired functionalities.

Keywords Core-shell · ZrO$_2$/polmer nanocomposites · Sol–gel method · Polymerization

Introduction

The strategy for designing and fabricating organic–inorganic nanocomposite particles has attracted considerable attention because of their novel and enhanced properties, including mechanical, chemical, optical, rheological, and electrical properties [1–4]. A variety of methods have been demonstrated for generating nanocomposite particles in the past decades. Some investigators reported that such nanocomposites could be prepared by encapsulation of inorganic particles in a polymer shell [5, 6], in which the effect of compounding was closely related to the dispersion stability of inorganic particles in polymerized media. The monodispersed suspension of inorganic nanoparticles is, however, not easily obtained because of its high surface energy in organic solvents and/or polymer media, which results in a wide distribution of particles finally. To overcome the difficulty in obtaining homogenous dispersion of inorganic particles, the sol–gel technique is commonly used for the synthesis of organic–inorganic advanced materials, which can offer the possibility to design nanocomposite structure at a molecular level. Recently, the emulsion copolymerization method has been widely used for the synthesis of hybrid nanoparticles such as SiO$_2$/polymer [7–10], and TiO$_2$/polymer [11–13] by chemically modifying the sol of metal oxides. Such an approach could provide a facile access to the preparation of shape/size-controlled nanocomposites. In our previous study [9], the core-shell SiO$_2$/PAA/PS nanoparticles were synthesized through the combination of sol–gel method and a dispersed polymerization approach, where the functional silica particles structured with vinyl groups on their surfaces were synthesized by the hydrolysis and polycondensation of tetraethoxysilane. The vinyltriethoxysilane (VTEOS) was used as a silane agent to form cores which were used as

J. Wang · T. J. Shi (✉)
School of Chemical Engineering, Hefei University of Technology, Hefei 230009, People's Republic of China
e-mail: stjhfut@163.com

X. C. Jiang
School of Materials Science & Engineering, University of New South Wales, Sydney, NSW 2052, Australia

seeds to copolymerize with styrene and acrylic acid to form SiO$_2$/PAA/PS nanoparticles. In comparison with the transition metal alkoxides such as VTEOS and Ti(OBt)$_4$, the hydrolysis and condensation reactions of zirconium alkoxides (Zr(OPr^n)$_4$) are too active to be controlled in the preparation of ZrO$_2$/polymer core-shell nanoparticles, although they have shown interesting functional properties and potential applications in many areas[14]. To achieve hybrid ZrO$_2$ nanocomposites, strong complexing ligands were commonly used as stabilizing agents for non-silicate metal alkoxides precursors [15]. The commonly used chelating ligands could be β-diketones and allied derivatives such as polyhydroxylated polyols and α- or β-hydroxyacids. It was recently found that the acetoacetoxyethylmethacrylate (AAEM) could act both as a strong chelating agent and a highly reactive methacrylate group, which, therefore, readily polymerize with the other vinyl monomers through chemical bonds. Moreover, the emulsifier-free emulsion polymerization has been proved to effectively eliminate the shortcomings of emulsifier that could lead to negative effects on the material properties [16, 17], and it is a potentially practical method in preparing environmentally friendly core-shell nanoparticles. During the polymerization, the use of polar solvent and another hydrophilic monomer would be helpful to increase the rate of polymerization and stability of emulsion [18]. However, the details in nucleation and growth of hybrid ZrO$_2$ nanocomposites, and their thermal stability need to be further understood. Therefore, the development of facile and effective approaches to obtain the desired hybrid ZrO$_2$ nanocomposites and further understanding on the formation mechanism is a still challenging task.

In this study, the core-shell ZrO$_2$/PAAEM/PS nanoparticles were synthesized through the combination of a sol–gel method and an emulsifier-free emulsion polymerization approach. The microstructure and composition of the as-prepared nanocomposites were characterized by using various advanced techniques such as transmission electron microscopy (TEM) and X-ray diffractometer (XRD). The interactions between inorganic and organic components are then measured by Fourier transform infrared spectroscopy (FTIR) and X-ray photoelectron spectroscopy (XPS) techniques. The thermal gravimetry analyzer (TGA) technique is finally used to check and evaluate the thermal stability of the hybrid core-shell nanoparticles.

Experimental

Materials

Zirconium propoxide (Zr(OPr^n)$_4$) (70% in propanol) and AAEM (99%) were provided by Aldrich Co. and Eastman Co. (USA), respectively. Propanol (PrOH) was obtained from Shanghai Reagent Co. (Shanghai, China). Styrene (St, chemically pure grade) and potassium persulphate (KPS, chemically pure grade) used as initiators in this study, were purchased from Tianjin Chemical Factory (Tianjin, China), and all the monomers were purified prior to use.

Preparation of AAEM-Modified ZrO$_2$ Sol

Zr(OPr^n)$_4$ and AAEM were used as precursors and a functionalized chelating ligand in the preparation of AAEM–ZrO$_2$ sol. The molar ratios of Zr(OPr^n)$_4$/AAEM/H$_2$O/PrOH were fixed at 1:1:10:30 in the reaction system. The hydrolysis and polycondensation of the AAEM-modified precursor of Zr(OPr^n)$_4$ were conducted in a conical flask equipped with magnetic stirrer, dropping funnels, and inlet for nitrogen gas. The reaction was carried out for ~8 h at room temperature. The AAEM-modified ZrO$_2$ sol was finally obtained.

Preparation of ZrO$_2$/PAAEM/PS Nanoparticles

ZrO$_2$/PAAEM/PS hybrid nanoparticles were prepared through the polymerization of the emulsifier-free emulsion process. The AAEM-modified ZrO$_2$ cores were used for seeds in the formation of ZrO$_2$/PAAEM/PS hybrid nanoparticles by copolymerizing with styrene. In this polymerization process, the mixture of distilled water and PrOH were used as the reaction medium, and three steps were involved in a typical synthesis. First, an appropriate amount of KPS (2 wt% based on monomer), AAEM-modified ZrO$_2$ sol, and AAEM (used as the second monomer, the molar ratio of AAEM/St is 0.2) were added into the reactor, followed by stirring to make sure the mixture was homogeneous, along with the heating up to 80 °C. Then the styrene monomer was added dropwise into the mixed solution. The polymerization was carried out for 4 h further after the feeding was finished. Finally, the reaction solution was naturally cooled down to room temperature. The product was separated by centrifugation and completely rinsed by water and alcohol respectively for further characterization. The blank sample of PAAEM/PS nanoparticles was also prepared by means of the similar emulsifier-free polymerization approach.

Characterization

The morphology and size of the as-prepared hybrid nanoparticles was checked through a H-800 Transmission Electron Microscopy (TEM) (Hitachi Co., Japan). X-ray diffraction (XRD) analysis was performed on a D/max-γB X-ray Diffractometer (Rigaku, Japan) with graphite-monochromatized CuKα radiation ($\lambda = 1.54178$ Å). The

interaction between inorganic core and organic shell was examined by FTIR operated on an IR-200 (Thermo Electron Co., U.S.). Thermal-gravimetry analysis (TGA) was conducted on a Pyrisl analyzer (PE Co., USA) at a heating rate of 10 °C/min under nitrogen protection. The elements of the hybrid nanoparticles were analyzed on VG model Escalab 250 X-ray photoelectron spectroscope (Thermo. Electron, USA).
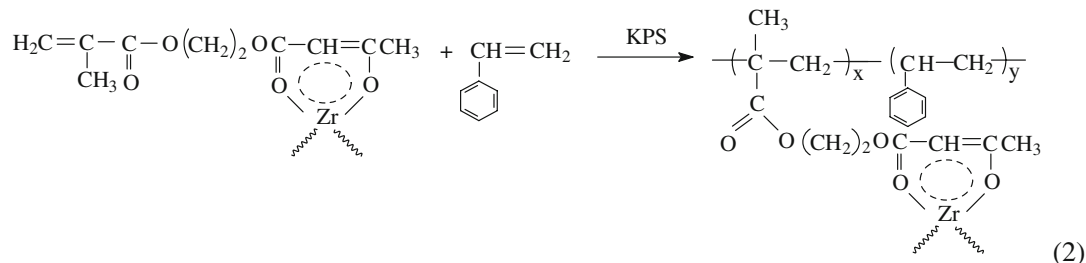
Results and Discussion

Core-shell ZrO$_2$/PAAEM/PS Particles

AAEM-modified ZrO$_2$ sol was prepared by the hydrolysis and polycondensation of Zr(OPr)$_4$. The chelating reaction between AAEM and Zr(OPr)$_4$ in propanol was described in a scheme as below:

$$H_2C=C-C-O(CH_2)_2\,OCCH_2CCH_3 \; + \; Zr(OPr^n)_4 \xrightarrow{\;H_2O\;} H_2C=C-C-O(CH_2)_2\,OC-CH=CCH_3 \tag{1}$$
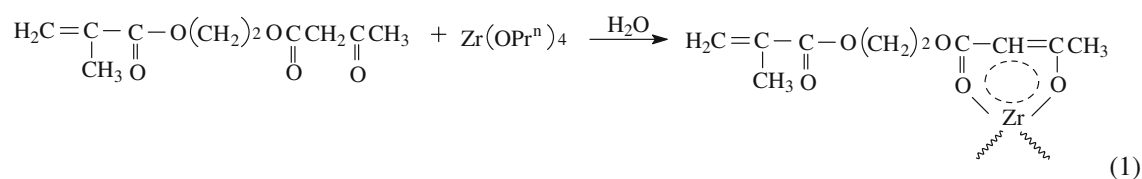
where the AAEM molecule plays the dual roles: (i) of providing chelating bonds for combining with Zr(OPr)$_4$ that could control the hydrolysis rate of Zr(OPr^n)$_4$, and (ii) of providing double bonds for copolymerizing with the other vinyl monomer in the formation of an organic shell. This would make significant contribution to enhance the mechanical and thermochemical properties of the hybrid microspheres. At the second stage, the AAEM-modified ZrO$_2$ sol reacted with the styrene monomer to form a polymer shell around ZrO$_2$ core, and the reaction equation could be briefly summarized as below:

$$\tag{2}$$

TEM image of the ZrO$_2$/PAAEM/PS hybrid nanoparticles. They are spherical in shape and the particle surface seems smooth with a diameter of ca. 250 nm and a shell thickness of ca. 25 nm. An obvious contrast between the core and the shell of the latex particles could be observed in Fig. 1, which is possibly caused by the difference of electron penetrability to the inorganic core and the organic shell. Furthermore, the inorganic ZrO$_2$ cores were entirely covered by the polymer, suggesting that the AAEM could modify ZrO$_2$ homogeneously. A close inspection to the core-shell particles reveals that the core-shell composite particles are of spherical shape with nearly uniform size, although the size of these ZrO$_2$ cores is not very uniform as shown in the TEM image.

XRD Analysis

The variety of phases of PAAEM/PS and ZrO$_2$/PAAEM/PS nanoparticles were investigated by XRD technique.

Figure 2 shows a broad peak around $2\theta = 20°$ in the XRD pattern (1) of the PAAEM/PS, corresponding to the typical characteristic of amorphous polymer. The XRD pattern (2) of ZrO$_2$/PAAEM/PS nanoparticles also shows a broad peak around $2\theta = 20°$ indicating that the hybrid nanocomposites are amorphous. The peak half-width of ZrO$_2$/PAAEM/PS nanoparticles becomes broader, suggesting that the inorganic component (ZrO$_2$) has interpenetrated with organic polymer chains to be compatible with each other; otherwise, two separate XRD diffraction domains could be found [19].

Microstructure of Nanocomposites

The morphology and size of the core-shell nanocomposites was characterized by TEM technique. Figure 1 shows the

FTIR Spectrum Analysis

To further investigate the bonding characteristics or the interaction between the inorganic core and the polymer

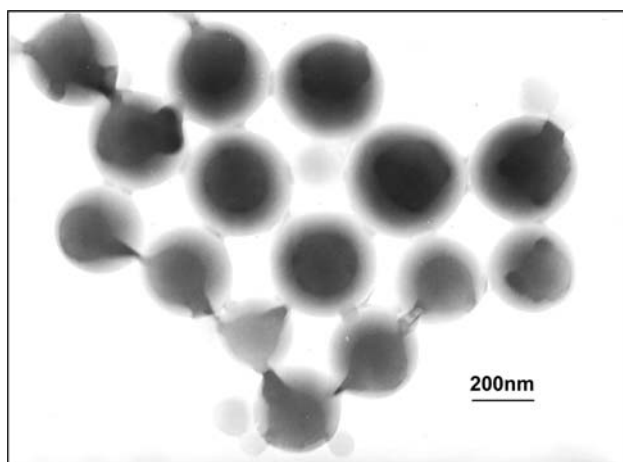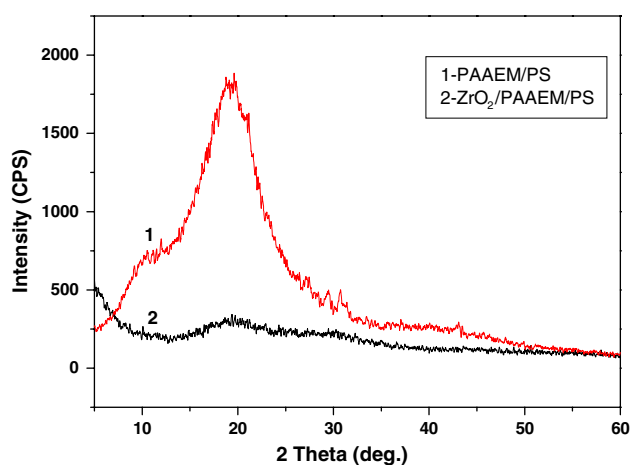**Fig. 1** TEM image of ZrO$_2$/PAAEM/PS hybrid nanoparticles

Fig. 2 XRD patterns of (1) PAAEM/PS nanoparticles; and (2) ZrO$_2$/PAAEM/PS hybrid nanoparticles
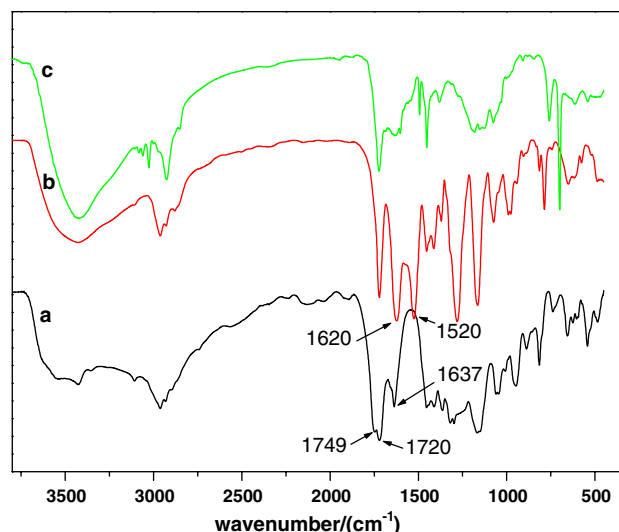

Fig. 3 Infrared spectra of **a** AAEM; **b** AAEM-modified zirconium propoxide; and **c** PS/PAAEM/ZrO$_2$ hybrid nanoparticles

vibration of the enolic form of β- cetoesters [20]. This could lead to a conclusion that the chelating reaction between zirconium atoms and AAEM groups occurred. In comparison with the free AAEM monomer, the stretching vibration of ester group at $\sim 1,749$ cm^{-1} was not observed in the AAEM-modified zirconium propoxide sol, suggesting that most of the AAEM monomers were bonded to zirconium atoms. As a result, the chemical bonds were formed between the zirconium oxo-polymers and the methacrylate monomer. The broad band located in the range of 300–600 cm^{-1} could be assigned to the stretching vibration of Zr–O–Zr of the AAEM-modified zirconium propoxide (Fig. 3b), and the ZrO$_2$/PAAEM/PS nanocomposite (Fig. 3c), respectively.

Considering the hybrid nanocomposites, the absorption peaks in FTIR spectra located at around 1,600 cm^{-1}, 1,494 cm^{-1}, and 1452 cm^{-1} could be attributed to the stretch vibrations of benzene ring, whereas those located at around 760 cm^{-1} and 698 cm^{-1} could be attributed to the banding vibrations of benzene ring originated from polystyrene. In addition, the intensity of the characteristic absorption peak of C=C located at $\sim 1,637$ cm^{-1} decreased remarkably in comparison to thaht of the AAEM monomer, indicating that the styrene monomer copolymerized with the vinyl groups of the AAEM-modified zirconium propoxide. It was also noted that the characteristic C=C peak located at $\sim 1,637$ cm^{-1} (Fig. 3b) decreased remarkably in comparison to that of the AAEM monomer, which is because of the effect of the strong vibration peak located at 1,620 cm^{-1} in the AAEM-modified zirconium sole [20]. The results are well in agreement with our proposed molecular-designed reaction process (see Eqs. 1 and 2).

shell, the FTIR technique was used to characterize the organic groups among them. Figure 3 shows the typical infrared spectra of AAEM, AAEM-modified zirconium propoxide, and ZrO$_2$/PAAEM/PS hybrid nanoparticles. The polymers and the core-shell structures exhibit the characteristic stretching peaks of C–H (CH$_2$) at $\sim 2,960$ cm^{-1} and 2,875 cm^{-1}, as well as the distortion vibration peak of CH$_2$ centered at $\sim 1,460$ cm^{-1} and $\sim 1,410$ cm^{-1}, respectively. The stretching vibration bands centered at $\sim 1,749$ cm^{-1} and $\sim 1,720$ cm^{-1} (Fig. 3a) could be attributed to C=O stretching vibration of the ester group and keto group, respectively.

Further FTIR analysis provides more information about the microstructure of the core-shell nanostructures. Strong vibration peaks located at $\sim 1,620$ cm^{-1} and $\sim 1,520$ cm^{-1} appear in the FTIR spectrum of the AAEM-modified zirconium precursor, which correspond to the ν(C=O+C=C)

XPS Spectrum Analysis

The binding energies of Zr atoms with others from polymers were checked by using XPS spectrum. Figure 4 shows the XPS spectra of the core-shell ZrO₂/PAAEM/PS nanocomposites. A full-scan spectrum (Fig. 4a) reveals the strong characteristic signals of carbon and oxygen, as well as a weak signal of zirconium. The binding energies of 182.9, 284, and 532 eV could be attributed to Zr3d, C1s, and O1s peaks, respectively. In order to obtain more detailed information about the nanocomposites, the high-resolution spectra of the particular regions were further investigated and shown in Fig. 4b–d. The Zr3d spectra were characterized by doublet terms of Zr3d$_{3/2}$ and Zr3d$_{5/2}$ due to spin-orbit coupling (Fig. 4b), and the 2.4 eV energy difference was found between Zr3d$_{3/2}$ and Zr3d$_{5/2}$, which is in good agreement with the reported values for ZrO₂ samples [21]. Such binding energy analysis suggested the formation of zirconium(IV) oxides in the nanocomposites. The binding energy of the Zr3d$_{5/2}$ band (ca. 182.9 eV) in the hybrid particles was found to be higher than that in ZrO₂ (ca. 182.2 eV), suggesting that the binding energy between zirconium nucleus and inner electrons was changed, and the chemical bond could probably form between the inorganic cores and the organic components.

A broad and complex band for O1s was observed in the XPS spectrum (Fig. 4c) for the hybrid nanoparticles. A better fit of the spectrum along with baseline-corrected raw data revealed the convolution of four different groups. The first band O$_I$ located at ∼530.4 eV corresponds to the O1s of Zr–O bond. The O$_2$ band centered at ∼532.3 eV could be ascribed to the O1s in C–O group. The O$_3$ and O$_4$ energy bands located at around 533.6 and 534.3 eV could be assigned to the O1s in C=O associated with aliphatic chain and conjugate ring, respectively. The slight higher binding energy for the O1s in C=O of the conjugate ring was due to the coordination of organic ligand [22]. Moreover, the C1s peak was also fitted and five bands were obtained as shown in Fig. 4d. The peaks located at ca. 284.6, 286.5, and 289.0 eV could be ascribed to the C–H, C–O and C=O of polymers, respectively. Due to the complicated core-shell nanocomposites and the limitation of XPS technique in thickness detection, it is believed that more study needs to be performed to further understand the core-shell nanocomposites.

Thermal Stability

The thermochemical property of the PAAEM/PS nanoparticles and ZrO₂/PAAEM/PS hybrid nanoparticles was measured by TGA technique. The weight loss starting at around 260 °C, as shown by the TGA curves (Fig. 5), could be attributed to the decomposition of molecular chain of PAAEM. The TGA curve (1) of PAAEM/PS nanoparticles shows the maximum weight loss rate occurred at ∼430 °C, while the maximum weight loss rate for the ZrO₂/PAAEM/PS hybrid nanoparticles is located at ∼447 °C. This could also be supported by difference

Fig. 4 XPS spectra of ZrO₂/PAAEM/PS hybrid nanoparticles: **a** a full-scan XPS spectrum of the hybrid nanoparticles; **b** Zr3d signals for the nanoparticles; **c** deconvolution of O1s signal for the nanoparticles; and **d** deconvolution of C1s signal for the nanoparticles
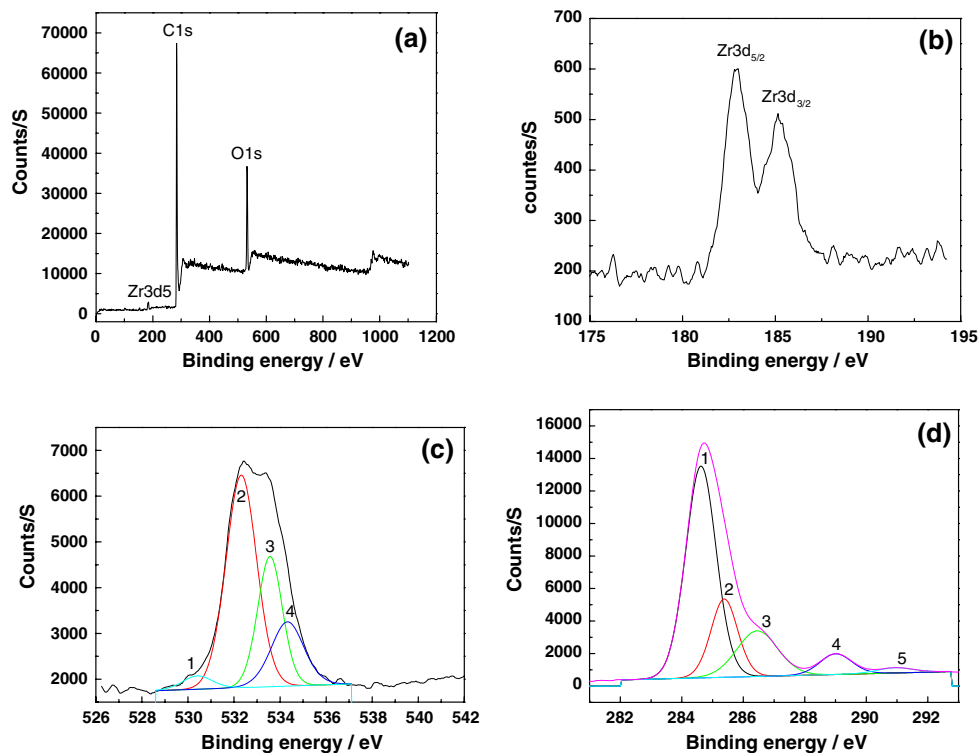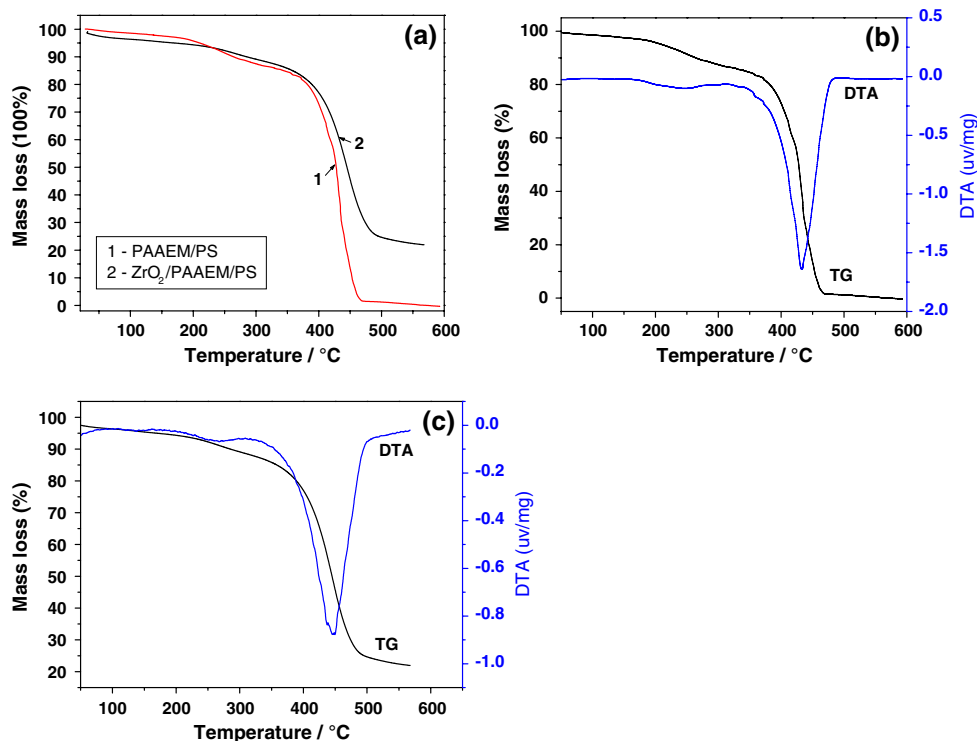
Fig. 5 **a** TGA curves of (1) PAAEM/PS nanoparticles and (2) ZrO$_2$/PAAEM/PS hybrid nanoparticles; **b** DTA curve of PAAEM/PS nanoparticles; and **c** DTA curve of ZrO$_2$/PAAEM/PS hybrid nanoparticles clearly showing the decomposition temperature of the hybrid nanocomposites

thermal analysis (DTA) curves shown in Fig. 5b, c. These results indicate that the hybrid nanocomposites have a better thermal stability than pure polymer particles. It can be assumed that the crosslink points between the inorganic core and the polymer shell played a key role in stabilizing the hybrid nanocomposites. The network formed by inorganic and organic molecules may restrain the movement of polymer chains. In addition, the content of the inorganic ZrO$_2$ in the hybrid nanocomposites was estimated to be around 20 wt% from the TGA thermogram (Fig. 5a). The chemical elemental analysis of the core-shell nanocomposites is under progress, and the results will be reported in our future study.

Conclusion

This study developed a facile and effective approach to prepare the core-shell ZrO$_2$/PAAEM/PS hybrid nanoparticles through a combined sol–gel approach and emulsifier-free emulsion polymerization. The hydrolysis and condensation of zirconium propoxide could be readily controlled by chelating with AAEM monomer. The chemical bonds between organic and inorganic materials formed by means of a highly reactive methacrylate group of AAEM have been confirmed by XRD, FTIR, XPS, and TGA analysis, which would benefit not only for the formation of core-shell hybrid nanoparticles but also for enhancing the thermal stability. The findings would be

useful for the synthesis of shape/size-controlled hybrid nanocomposites with desired functional properties.

References

1. M.P. Gispert, A.P. Serro, R. Colaco, B. Saramago, Wear **260**, 149–158 (2006). doi:10.1016/j.wear.2004.12.040
2. Y. Oaki, H. Imai, Adv. Mater. **18**, 1807–1811 (2006). doi: 10.1002/adma.200600531
3. H.M. Xiong, Z.D. Wang, D.P. Liu, J.S. Chen, Y.G. Wang, Y.Y. Xia, Adv. Funct. Mater. **15**, 1751–1756 (2005). doi:10.1002/adfm.200500167
4. A.R. Mahdavian, Y. Sehri, H. Salehi-Mobarakeh, Eur. Polym. J. **44**, 2482–2488 (2008). doi:10.1016/j.eurpolymj.2008.05.025
5. D.G. Yu, J.H. An, J.Y. Bae, S. Kim, Y.E. Lee, S.D. Ahn, S.Y. Kang, K.S. Suh, Colloids Surf. A Physicochem. Eng. Asp. **245**, 29–34 (2004). doi:10.1016/j.colsurfa.2004.06.026
6. G.Y. Liu, X.L. Yang, Y.M. Wang, Polymer **48**, 4385–4392 (2007). doi:10.1016/j.polymer.2007.05.060
7. L.Y. Hao, C.L. Zhu, C.N. Chen, P. Kang, Y. Hua, W.C. Fan, Z.Y. Chen, Synth. Met. **139**, 391–396 (2003). doi:10.1016/S0379-6779(03)00193-0
8. J. Zhou, S.W. Zhang, X.G. Qiao, X.Q. Li, L.M. Wu, J. Polym. Sci., Part A: Polym. Chem. **44**, 3202–3209 (2006). doi:10.1002/pola.21434
9. H.L. Wang, T.J. Shi, L.F. Zhai, J. Appl. Polym. Sci. **102**, 1729–1733 (2006). doi:10.1002/app.24354
10. L. Jakuczek, J.S. Gutmann, B. Müller, C. Rosenauer, D. Żuchowska, Polymer (Guildf) **49**, 843–856 (2008). doi:10.1016/j.polymer.2007.12.030

11. A.D. Gianni, S. Trabelsi, G. Rizza, M. Sangermano, H. Althues, S. Kaskel, B. Voit, Macromol. Chem. Phys. **208**, 76–86 (2007). doi:10.1002/macp.200600431

12. Y. Rong, H.Z. Chen, G. Wu, M. Wang, Mater. Chem. Phys. **91**, 370–374 (2005). doi:10.1016/j.matchemphys.2004.11.042

13. H.L. Luo, J. Sheng, Y.Z. Wan, Mater. Lett. **62**, 37–40 (2008). doi:10.1016/j.matlet.2007.04.108

14. A. Hernández Battez, R. González, J.L. Viesca, J.E. Fernández, J.M. Díaz Fernández, A. Machado, R. Chou, J. Riba, Wear **265**, 422–428 (2008). doi:10.1016/j.wear.2007.11.013

15. J.F. Huang, *Sol–gel Principle and Technology* (Chemical Industry Press, Beijing, 2005)

16. X.J. Cui, S.L. Zhong, H.Y. Wang, Polymer **48**, 7241–7248 (2007)

17. N.V. Dziomkina, M.A. Hempenius, G.J. Vancso, Eur. Polym. J. **42**, 81–91 (2006)

18. G.H. Ma, Z.G. Su, *Polymer Microspheres* (Chemical Industry Press, Beijing, 2005)

19. I.S. Elashmawi, N.A. Hakeem, E.M. Abdelrazek, Physica B **403**, 3547–3552 (2008). doi:10.1016/j.physb.2008.05.024

20. Z.M. Wang, X.X. He, *Infrared Absorption Spectroscopy* (Oil Industry Press, Beijing, 1982)

21. M. Alvarez, T. López, J.A. Odriozola, M.A. Centeno, M.I. DomÍnguez, M. Montes, P. Quintana, D.H. Aguilar, R.D. González, Appl. Catal. B **73**, 34–41 (2007). doi:10.1016/j.apcatb.2006.12.010

22. D. Briggs, *Handbook of X-ray and Ultraviolet Photoelectron Spectroscopy* (Heyden & Son Ltd, United Kingdom, 1977)